

Temperature dependence of the electron-hole-liquid luminescence in Si[†]

R. B. Hammond, T. C. McGill,* and J. W. Mayer

California Institute of Technology, Pasadena, California 91125

(Received 25 August 1975)

Detailed measurements and line-shape fits of the combined LO- and TO-phonon assisted electron-hole condensate luminescence lines from laser-excited, high-purity Si are reported in the temperature range from 2.2 to 13.0°K. These data permit a determination of the liquid density n , chemical potential μ , the Fermi energy E_F , and the work function ϕ , as functions of temperature. Fitting of these data to the T^2 dependence expected from Fermi-liquid theory gives $n(T) = [3.33 \pm 0.03 - (1.5 \pm 0.5) \times 10^{-3} T^2] \times 10^{18} \text{ cm}^{-3}$; $\mu(T) = [(1088.7 \pm 0.1) + \hbar\omega_{\text{ph}}^{\text{TO}} - (5.9 \pm 1.1) \times 10^{-3} T^2] \text{ meV}$; $E_F(T) = [22.2 \pm 0.1 - (8.0 \pm 2.2) \times 10^{-3} T^2] \text{ meV}$; and $\phi(T) = [8.21 \pm 0.1 + (5.9 \pm 8.2) \times 10^{-3} T^2] \text{ meV}$, where T is in degrees Kelvin, and $\hbar\omega_{\text{ph}}^{\text{TO}}$ is the energy of the TO phonon assisting in the recombination. Analysis of the temperature dependence of the density gives a value for the second derivative of the ground-state energy per pair with respect to a density of $4.9 \times 10^{-37} \text{ meV cm}^6$. The value of the density and work function at zero temperature, and the values of the coefficients of the various T^2 terms are compared with various theoretical calculations.

I. INTRODUCTION

The condensation of nonequilibrium electrons and holes into high-density metallic electron-hole droplets at temperatures $\lesssim 6^\circ \text{K}$ in high-purity Ge single crystals has been demonstrated by a wide variety of experiments.¹⁻⁷ The properties of this electron-hole plasma, first predicted by Keldysh,⁸ have been quite thoroughly studied. Using a simple model for the luminescence line shape of electrons and holes recombining from this condensed phase,¹ Thomas *et al.*^{2,9} have determined the density of the electron-hole liquid between 1.08 and 6.5°K. Their results give condensate densities between 2.4 and $0.8 \times 10^{17} \text{ cm}^{-3}$ with a monotonically decreasing density for increasing temperature. The calculated line shape agrees closely with the experimental line shape over this range of temperatures. Besides the condensate density, this line-shape fitting procedure yields values for the chemical potential and Fermi level of the condensate. Thomas *et al.*² were able to show that within experimental error the chemical potential and the Fermi level for the electron-hole liquid in Ge have the T^2 dependences expected from Fermi-liquid theory.

Although the condensation of nonequilibrium electrons and holes into metallic electron-hole droplets has been observed in Si,¹⁰⁻¹² experimental investigations of this phenomenon have not been as extensive as in Ge. A single qualitative fit of the condensate luminescence line shape in Si was reported by Pokrovsky *et al.*¹¹ and yielded a density of $3.7 \times 10^{18} \text{ cm}^{-3}$ for the electron-hole condensate at 4.2°K. Using this same luminescence line shape from Pokrovsky *et al.*,¹¹ other investigators^{13,14} have estimated the condensate-exciton-gas work function to be approximately 7 meV.

The particular phonon-assisted recombination line published by Pokrovsky *et al.*¹¹ consists of two closely spaced phonon-assisted lines, produced by the TO and LO phonons. However, for simplicity and a lack of knowledge of the ratio of the two components, they assumed that the recombination line was made up of a single line due to the TO phonon. This assumption leads to an overestimate of the condensate density and an underestimate of the work function. These results have not been extended to obtain the accurate values of the density, work function, Fermi energy, and chemical potential or the variation of these parameters with temperature.

The purpose of this work is to exploit the simple single-particle model of the line shape to obtain accurate values of the parameters which characterize the electron-hole liquid in Si. We have included the effects of both the TO- and LO-phonon replicas in our analysis of the condensate luminescence. We have analyzed Si photo luminescence spectra between 2.2°K and 13°K and determined the condensate density, chemical potential, Fermi level, and work function in this temperature range. We find that the variation with temperature of these parameters is consistent with the metallic plasma model for the condensate in Si and obtain values of the parameters characterizing the temperature dependence which are in approximate agreement with the theoretical estimates of Vashishta, Das, and Singwi.¹⁵

II. EXPERIMENTAL

The photoluminescence experiment was performed on *b*-type single-crystal Si slices with net acceptor concentrations of $N_A - N_D = 1.5 \times 10^{11}$ and $7 \times 10^{11} \text{ cm}^{-3}$. The higher-purity crystal, on which all the line-fitting data were taken, was

10×20×3 mm thick and was laser excited in the middle of a 10×20-mm face which was mechanically polished and chemically etched. The sample temperature was controlled in a Janis variable-temperature He Dewar and measured with a Ge resistance thermometer in contact with the Si sample. For laser excitation, a GaAs laser mounted inside the Dewar 4 mm above the sample surface produced a circular excitation spot on the sample of ~0.5 mm in diameter. To minimize heating in the Si, the laser was pulsed with 2-μsec pulses at a repetition rate of 20 kHz. Instantaneous optical powers of 0.3–3.0 W were used. The Si luminescence was analyzed with a Spex 1400-II double-grating spectrometer, detected with a RCA 7102 S-1 photomultiplier tube operated at 195°K, and the electrical signal was processed with a lock-in amplifier and recorded on a strip-chart recorder. The combined detector sensitivity and spectrometer transmission were determined by measuring the intensity as a function of wavelength for radiation from a blackbody at 2425°K. At wavelengths in the range studied here, the blackbody radiation from this source is relatively independent of wavelength. The spectrometer broadening was determined by measuring the width of a number of narrow lines from a Hg lamp which appear in the wavelength range used here. These effects were then included in the calculated line shapes. The absolute energy position of the spectrometer was calibrated using the very sharp (<1 Å) luminescence line from a Hg lamp at 1.1287 μm.

III. SILICON LUMINESCENCE SPECTRA

Si photoluminescence spectra at low temperatures consist of a number of different lines arising from electrons and holes recombining from states such as free excitons, excitons bound to impurities, and electron-hole condensate. Here we are primarily concerned with free-exciton and condensate emission. Since Si is an indirect band-gap semiconductor, radiative recombination is accompanied by phonon emission. There are two dominant phonon-assisted recombination processes which emit longitudinal-optical (LO) and transverse-optical (TO) phonons, respectively. The recombination radiation spectrum is thus composed of two replicas separated by the TO-LO splitting of ~2 meV.¹⁶ To discuss the calculations, then, it is appropriate to present an experimental spectrum which illustrates the main features of this strong free-exciton and condensate luminescence in Si. Such a spectrum is shown in Fig. 1 for laser excitation at 2.1°K. The free-exciton recombination radiation line that occurs at 1.097 eV in Fig. 1 is composed of the two phonon replicas due to TO- and LO- phonon emission, respectively. The in-

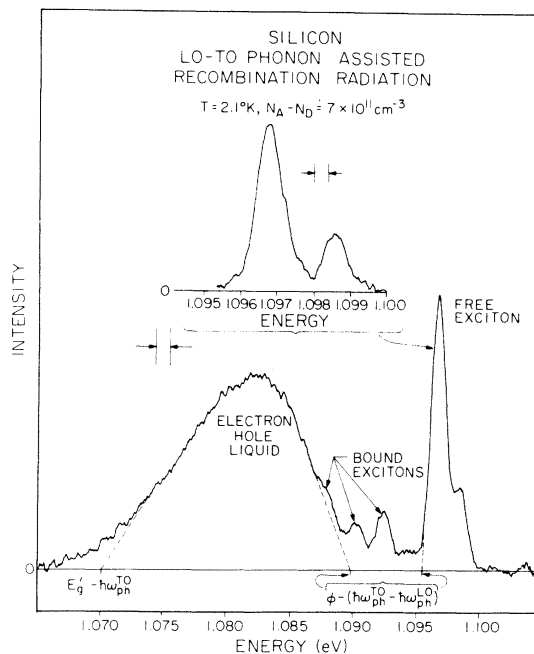


FIG. 1. LO- and TO-phonon-assisted recombination radiation spectrum from laser-excited high-purity Si at 2.1°K. The spectrum has strong free-exciton luminescence which can be resolved into its LO- and TO-phonon components. The LO- and TO-phonon-assisted condensate luminescence is a broad peak centered at 1.082 eV. The extrapolated low-energy threshold of this luminescence yields the value of the modified band gap for the condensate less the energy of the TO phonon. The magnitude of the separation of the extrapolated high-energy edge of the condensate line and the low-energy threshold of the free-exciton line is shown. This value corrected for the difference in the LO- and TO-phonon energies is approximately the condensate-exciton work function.

sert shown in the upper portion of Fig. 1 shows these replicas under high resolution. They are split by 1.8 meV and their intensity ratio is LO:TO = 0.33. In exciton absorption measurements, the observed ratio¹⁷ is LO:TO = 0.11. The ratio in luminescence is temperature dependent and approaches the ratio from absorption at high temperatures.¹⁸

The LO- and TO-phonon replicas also occur in the emission from the electron-hole condensate centered at 1.082 eV. However, owing to the intrinsic width of the condensate luminescence line (~12 meV), it is not possible to resolve the two replicas. On the other hand, since there are two superposed yet slightly split contributions to the condensate luminescence, the observed line shape is modified and also shifted in line position depending on the relative intensities of the two phonon replicas in the condensate emission. As outlined in Sec. IV, these considerations are important in determining the electron-hole-liquid density and

the liquid-gas work function. For example, to determine the work function a 1.8-meV correction must be added to the energy difference between the low-energy edge of the TO free-exciton line and the high-energy edge of the LO condensate line. This is an appreciable ($\sim 20\%$) correction to the work function.

The effective energy gap for the condensate is determined by the extrapolated threshold of the low-energy edge of the TO condensate line as shown schematically in Fig. 1. This extrapolation is accomplished by a line-fitting procedure discussed in Sec. IV. Also, in Fig. 1, three vertical arrows indicate the positions of bound-exciton complex lines. These lines have been observed previously.^{1,19,20} The doping levels of the samples studied previously were at least an order of magnitude higher than in the sample used to obtain the spectrum shown in Fig. 1. However, in the work reported below, it was necessary to use even higher-purity material to eliminate the influence of these extraneous lines.

IV. THEORETICAL LINE SHAPE

The basic concepts for the electron-hole-liquid line-shape calculation are shown schematically in Fig. 2.¹ In this diagram we have the conduction and valence bands which are displaced in k space. The effective band gap E'_g for the condensate is smaller than the one-electron band gap E_g owing to the strong interactions between electrons and holes in this high-density state. The bands are

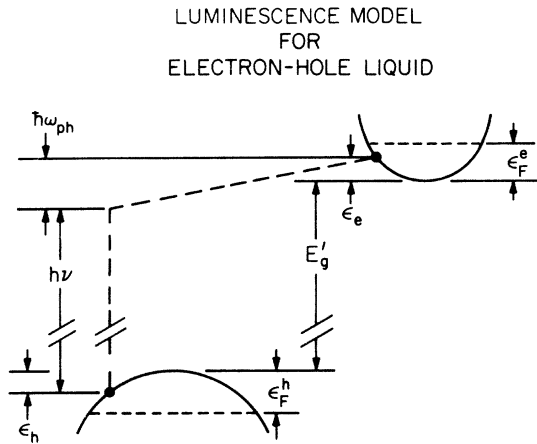


FIG. 2. Model for the radiative recombination of electrons and holes from the Fermi-degenerate electron-hole condensate. The valence and conduction bands are separated in energy and crystal momentum and are filled to their respective Fermi energies. E_g is the energy gap for the condensate. An electron with energy ϵ_e above the band minimum and a hole with energy ϵ_h above the band maximum recombine emitting a phonon with energy $\hbar\omega_{ph}$ and a photon with energy $h\nu$.

filled up to their respective quasi-Fermi levels (ϵ_F^e , ϵ_F^h) which are determined primarily by the condensate density but are also a weak function of the temperature. As shown in the diagram, an electron with energy ϵ_e may recombine with a hole of energy ϵ_h by emitting a phonon with energy $\hbar\omega_{ph}$ and a photon with energy $h\nu$. The lowest energy photon which can be emitted in such a recombination event is just $h\nu = E'_g - \hbar\omega_{ph}$ and occurs when an electron and a hole, each at its band extremum, recombine. On the other hand, the highest-energy photon which can be emitted is $h\nu = E'_g - \hbar\omega_{ph} + \epsilon_F^e + \epsilon_F^h$ which occurs when an electron and a hole, each at its respective quasi-Fermi level, recombine. Thus, the total width of the condensate luminescence line is approximately determined by the sum of the two quasi-Fermi levels, $\Delta h\nu = \epsilon_F^e + \epsilon_F^h = E_F$.

The line shape of luminescence, due to recombination of electrons and holes in the electron-hole liquid in Si, may be calculated for each phonon replica from

$$I_{\text{cond}}(h\nu) = A \int d\epsilon_e d\epsilon_h \rho_e(\epsilon_e) \rho_h(\epsilon_h) (e^{(\epsilon_e - \epsilon_F^e)/k_B T} + 1)^{-1} \times (e^{(\epsilon_h - \epsilon_F^h)/k_B T} + 1)^{-1} \delta(E'_g + \epsilon_e + \epsilon_h - \hbar\omega_{ph} - h\nu), \quad (1)$$

where ρ_e and ρ_h are the electron and hole density-of-states functions. The factor A contains the matrix elements for the transition and a number of other parameters, and, hence, is dependent on which phonon replica is being considered. This model assumes that (i) the energy-wave-vector relationship for the condensate is unmodified compared to the single-electron band structure (except for the decrease in band gap already mentioned); (ii) the matrix element for the recombination is independent of energy and crystal momentum; and (iii) the recombination is adequately described in a single-particle model. For convenience, in the calculation presented below we assume that the density of states varies as $\epsilon^{1/2}$.

With these assumptions, it is possible to calculate the form of one phonon replica. In Eq. (1) the value of $\hbar\omega_{ph}$ is the energy of the phonon which assists in the recombination. The quasi-Fermi levels are determined by the condensate density, the effective masses appropriate for the density of states, and the temperature.

In Si the strong luminescence line from the condensate is the sum of contributions from the LO- and TO-phonon replicas,

$$I_{\text{cond}}^{\text{TO+LO}}(E) = I_{\text{cond}}^{\text{TO}}(E) + I_{\text{cond}}^{\text{LO}}(E), \quad (2)$$

where each contribution is described by Eq. (1). To calculate the condensate luminescence line shape, it is necessary to know the relative intensity of these two contributions, i.e., we need

to know the ratio A_{LO}/A_{TO} . This ratio has recently been estimated to be the value obtained from exciton absorption¹⁸ of 0.11. We have chosen this ratio in the fits of the luminescence results reported in Sec. V. The energy splitting between the LO- and TO-phonon replicas was taken to be 1.8 meV.

To compare calculations of the LO- and TO-phonon-assisted electron-hole condensate luminescence according to Eq. (2) with experimental spectra, it is necessary to correct Eq. (2) for experimental distortions in the observed signal owing to detector sensitivity, spectrometer transmission, and spectrometer broadening. This was done in the calculations by first taking the calculated line shape of Eq. (2) and multiplying the result by the measured sensitivity-transmission function of our detector and spectrometer system. This line shape was then convolved with the measured spectrometer-broadening function to yield a line shape which we compared directly with experimental spectra.

The following steps were used to obtain a best fit to the condensate line shape and extract the condensate properties. (a) The temperature measured by the germanium resistance thermometer during the experiment was assumed correct. (b) The electron and hole quasi-Fermi energies were calculated for a range of densities. These quasi-Fermi energies depend directly on the density and also include a small T^2 temperature dependence at fixed density.²¹

$$E_F^e = \frac{\hbar^2}{2m_{de}} (3\pi^2 n)^{2/3} - \frac{\pi^2 m_{de} (k_B T)^2}{6\hbar^2 (3\pi^2 n)^{2/3}}, \quad (3a)$$

$$E_F^h = \frac{\hbar^2}{2m_{dh}} (3\pi^2 n)^{2/3} - \frac{\pi^2 m_{dh} (k_B T)^2}{6\hbar^2 (3\pi^2 n)^{2/3}}, \quad (3b)$$

where m_{de} and m_{dh} are the density-of-states effective masses for electrons and holes, respectively. The contribution to the densities of states from the six valleys in the silicon conduction band and the two valence bands are included in the definitions of the effective masses. The values of m_{de} and m_{dh} were taken to be $1.08m_e$ and $0.55m_e$, respectively.²² (c) Using the measured temperature and these calculated quasi-Fermi energies, the condensate luminescence line shape was calculated from Eq. (2) with the measured corrections due to the detector-spectrometer system. [Note that the condensate density enters Eq. (2) only through the quasi-Fermi energies. The temperature enters both through the quasi-Fermi energies and $k_B T$ in the denominators of the exponents.] (d) The line shapes calculated in this manner which yielded a best fit to the experimental line shape then gave a measure of the condensate density and quasi-Fermi energy. It is important to note that a best fit was achieved

without regard to the absolute energy position of the luminescence. That is, the value of $E_g' - \hbar\omega_{ph}^{TO}$ in Eq. (2) was not relevant to getting a best fit to the shape of the luminescence line and thus to determining the density and quasi-Fermi energy of the condensate. This procedure was made possible in practice because the sensitivity-transmission function for our detector-spectrometer combination was slowly varying over the energy range of interest. (e) After obtaining the best fit to the form of the line shape, the absolute energy position of $E_g' - \hbar\omega_{ph}^{TO}$ was extracted from the line fit. This value was then used to obtain the condensate chemical potential less the phonon energy:

$$\mu - \hbar\omega_{ph}^{TO} = E_g' - \hbar\omega_{ph}^{TO} + E_F, \quad (4)$$

where E_F is the sum of the electron and hole quasi-Fermi energies. (f) Finally, the exciton luminescence was fit to yield a value for the low-energy exciton threshold $E_{EX} - \hbar\omega_{ph}^{TO}$ using the procedure described in Ref. 18. The condensate-exciton work function was then calculated from the difference between the condensate chemical potential and the exciton threshold

$$\phi = (E_{EX} - \hbar\omega_{ph}^{TO}) - (\mu - \hbar\omega_{ph}^{TO}). \quad (5)$$

Local heating of the silicon sample by the incident laser beam could invalidate our assumption that the Ge sensor measured the appropriate temperature. To check for heating, we measured the dependence of the linewidth and line position of the condensate line for a number of different values of the incident laser power for temperatures between 2.2 and 9.0 °K. At temperatures higher than 9 °K, only the highest excitation levels produced the condensate radiation; so it was not possible to vary the excitation intensity. The condensate linewidths and line positions at different pump powers and different temperatures are summarized in Table I. At each temperature, these linewidths and line positions are unchanged (within the noise) at different excitation levels. This is evidence for the lack of heating in the experiment. Also for each temperature and excitation level, the value of the temperature was confirmed by fitting the free-exciton luminescence. In each case, the LO- and TO-phonon-assisted free-exciton luminescence agreed with the resistance thermometer measurement. At high temperatures, the width of the free-exciton luminescence is a good indicator of the temperature since kT broadening is large compared to the LO-TO splitting. On the other hand, at low temperatures where the kT broadening is small, the LO:TO intensity ratio is a strong function of temperature and is thus a sensitive measure of the temperature.¹⁷ These results rule out the possibility of local heating and justify our

TABLE I. Variation with laser excitation power of the linewidth and line position of the LO- and TO-phonon-assisted luminescence from the electron-hole condensate in Si.

Temperature (°K)	Laser, power ^a (W)	Electron-hole liquid full width at half-maximum (Å)	Electron-hole liquid line position ^b (μm)
2.2	0.3	125	1.1472
	0.6	124	1.1473
	1.5	124	1.1473
4.2	0.6	124	1.1473
	1.5	124	1.1474
	3.0	123	1.1473
7.0	0.3	124	1.1473
	0.6	124	1.1475
	1.5	124	1.1475
9.0	0.3	125	1.1475
	0.6	126	1.1476
	1.5	125	1.1475

For each temperature these numbers
are the same within the noise level.

^aLaser intensity is not corrected for the reflectance of Si.

^bLine position is measured as the midpoint of the half-maximum line.

use of the temperature as measured by the Ge sensor.

Before discussing the results, a brief discussion is appropriate at this point describing how the magnitude of the errors in the various condensate properties was determined. The errors in the density and the Fermi level were determined by finding the extremes of the condensate density which produced line shapes which obviously did

not fit the experimental spectra. The errors in the chemical potential and work function were less because the high-energy side of the condensate luminescence and also the exciton luminescence were fit quite precisely. Thus the accuracy in these parameters was limited only by the measurement procedure; that is, the energy accuracy in the spectrometer, detector, and signal processing. This accuracy was ± 0.1 meV.

V. RESULTS

The experimental spectrum for LO- and TO-phonon-assisted recombination and line fits for 4.2 °K are shown in Fig. 3. The line fit to the exciton spectrum, the sharp line at high energies, provides a verification that the temperature is 4.2 °K and gives a value for the threshold of

$$E_{EX} - \hbar\omega_{ph}^{TO} = 1.0969 \text{ eV}.$$

Fitting of the condensate line, the broad line at low energy, gives a value for the condensate density of

$$n(4.2 \text{ °K}) = 3.30 \times 10^{18} \text{ cm}^{-3}$$

and a value for the low-energy threshold of

$$E'_g(4.2 \text{ °K}) - \hbar\omega_{ph}^{TO} = 1.0665 \text{ eV}.$$

From these three experimental parameters and Eqs. (3)–(5), one obtains values for the sum of the quasi-Fermi energies

$$E_F(4.2 \text{ °K}) = 22.1 \text{ meV},$$

for the chemical potential

$$\mu(4.2 \text{ °K}) = 1.0886 \text{ eV} + \hbar\omega_{ph}^{TO},$$

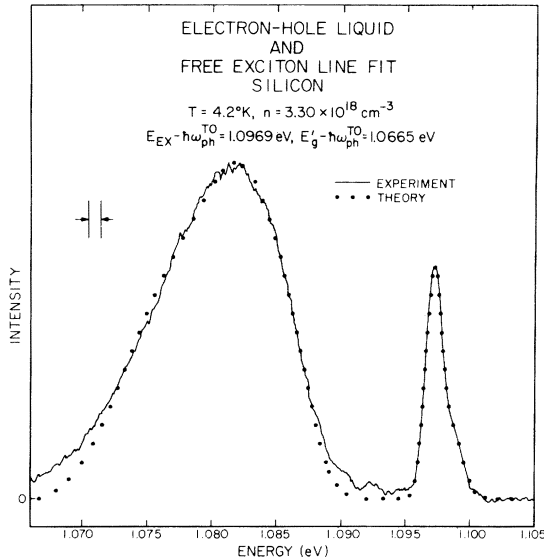


FIG. 3. Luminescence spectrum from high-purity Si at 4.2 °K. The LO- and TO-phonon-assisted recombination radiation from both the free-exciton and electron-hole condensate are shown. The results of line fits to the experimental lines are also shown.

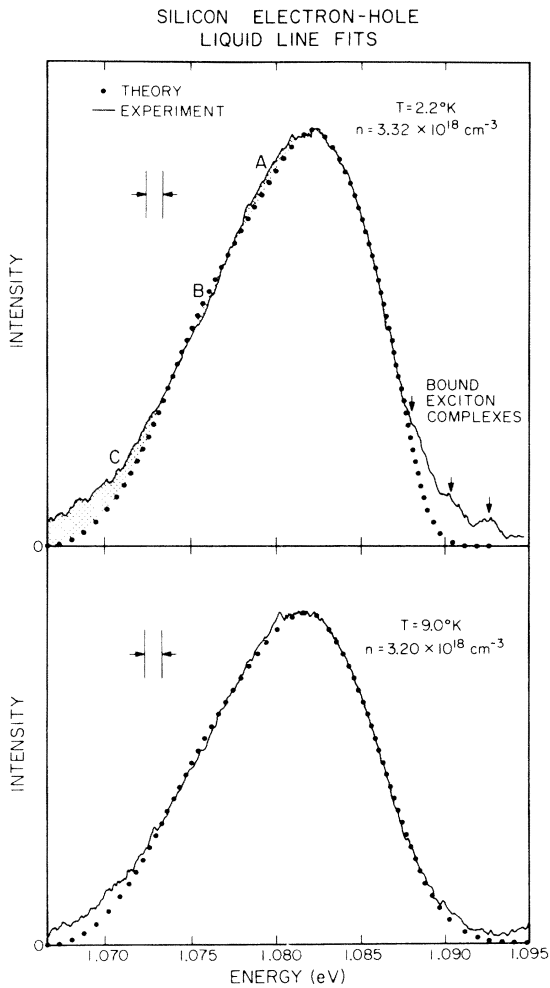


FIG. 4. LO- and TO-phonon-assisted recombination radiation from the condensate for laser excited high-purity Si at 2.2 and 9.0 °K, with a laser intensity of 600 mW. Calculated line fits (dotted lines) to this luminescence yield condensate densities of 3.32 and $3.20 \times 10^{18} \text{ cm}^{-3}$, respectively. Discrepancies between the calculated line shape and the experimental line shape at 2.2 °K are cross hatched and labeled A, B, and C. These same discrepancies can be seen at 9.0 °K, but they are diminished in size.

and for the work function

$$\phi(4.2 \text{ °K}) = 8.3 \text{ meV}.$$

Figure 4 shows line fits at two other temperatures of LO- and TO-phonon-assisted recombination radiation due to electrons and holes in the electron-hole condensate in Si. The condensate density is found to be $3.32 \times 10^{18} \text{ cm}^{-3}$ at 2.2 °K and $3.20 \times 10^{18} \text{ cm}^{-3}$ at 9.0 °K.

In the condensate line fit at 2.2 °K in Fig. 4, three regions of discrepancy between the calculation and the experimental line shape are shaded and labeled A, B, and C. These regions of dis-

crepancy were noted in the line fits at all temperatures and all excitation levels. The discrepancy region C is evidence of the recombination of electrons and holes with lower energy than is allowed in the simple band model. This discrepancy at low energy in the line fit has also been observed in Ge by several investigators^{2,9,22} and may be attributed to electrons and holes recombining from the condensate and leaving the condensate in an excited state, which is different from that given by the standard band model. Thus, the energy of the emitted photon is lowered by just the amount necessary to produce the excitation. The discrepancies between the calculated line shapes and the experimental spectra decrease continuously at higher temperature. This effect can be seen by comparing the fits at 2.2 and 9.0 °K for the electron-hole condensate as shown in Fig. 4.

At 2.2 °K (see Fig. 4) and 4.2 °K (see Fig. 3), weak lines due to recombination of excitons bound at impurity sites are observed on the high-energy side of the condensate line. This is the first reported observation of these lines in high-purity *p*-type Si ($N_A - N_D = 1.5 \times 10^{11} \text{ cm}^{-3}$). They are shown prominently in the luminescence spectrum of Fig. 1 for Si doped $7 \times 10^{11} \text{ cm}^{-3}$. For this work it was possible to reduce the intensity of these lines sufficiently that their effect on the line-shape fitting was not significant.

The quantitative results of the condensate luminescence line-shape fitting for Si are summarized in the graphs in Figs. 5–8. Qualitatively we see that the condensate density, Fermi level, and chemical potential each show a decrease with increasing temperature while the condensate-exciton work function increases with increasing tem-

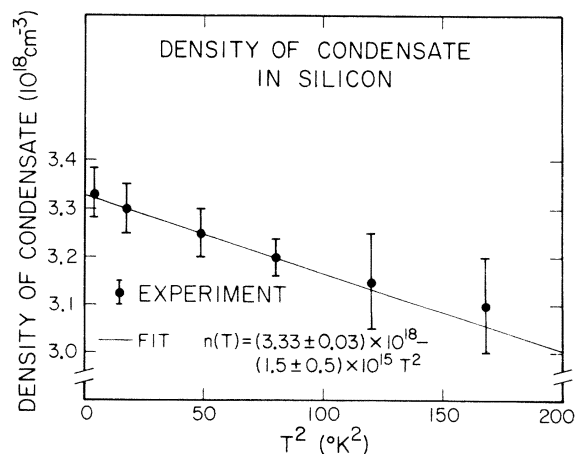


FIG. 5. Density of the electron-hole condensate vs temperature obtained by fitting the line shape of the LO- and TO-phonon-assisted recombination luminescence from the condensate in laser-excited Si.

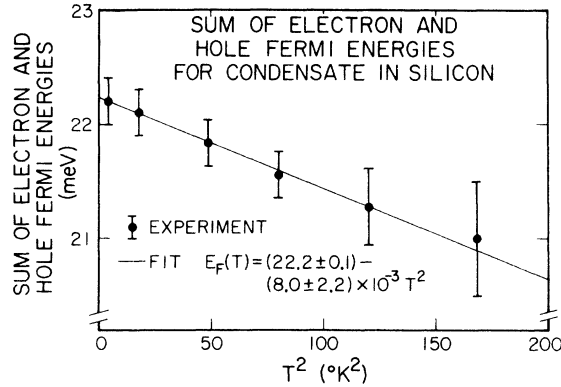


FIG. 6. Sum of the electron and hole Fermi energies vs temperature obtained by fitting the line shape of the LO- and TO-phonon-assisted recombination luminescence from the condensate in laser-excited Si.

perature. Since there was some contribution on the high-energy side of the condensate line from the free exciton at 11 and 13 °K, the error in the line-shape fits increased for these two temperatures above the error at lower temperatures.

The degenerate plasma model of the electron-hole condensate suggests the above noted trends. In fact, theoretically, we expect the following dependences on temperature^{2,15,23,24}

$$n(T) = n(0^\circ\text{K}) - \alpha T^2, \quad (6)$$

$$E_F(T) = E_F(0^\circ\text{K}) - \beta T^2, \quad (7)$$

$$\mu(T) = \mu(0^\circ\text{K}) - \delta T^2, \quad (8)$$

$$\phi(T) = \phi(0^\circ\text{K}) + \delta T^2, \quad (9)$$

where α , β , and δ are independent of temperature and because the one-electron band gap does not

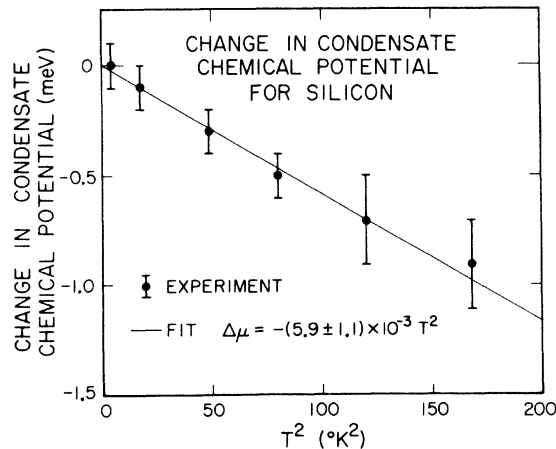


FIG. 7. Change in the chemical potential of the condensate with temperature obtained by fitting the line shape of the LO- and TO-phonon-assisted recombination luminescence from the condensate. The high-purity Si was excited by a laser.

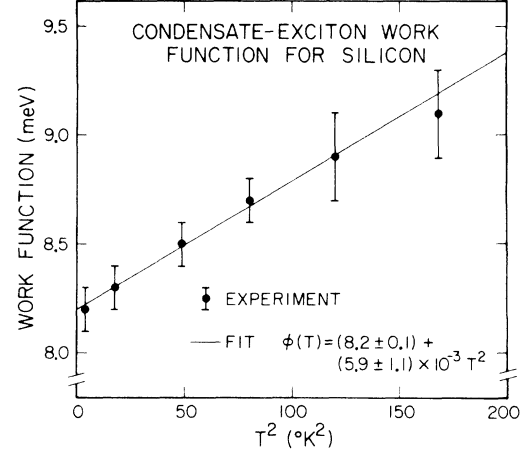


FIG. 8. Condensate-exciton work function vs temperature obtained by fitting the line shape of the LO- and TO-phonon-assisted recombination luminescence from the condensate in laser-excited Si.

change significantly ($\lesssim 0.1$ meV) in the temperature range 2–13 °K.²⁵

The coefficients of the T^2 term are the same for the chemical potential and the work function because the exciton binding energy is independent of temperature.

As shown in Figs. 5–8, the variation of each of the parameters is consistent with the T^2 dependences expected from theory. Fitting the data to the Eqs. (6)–(9), we obtain values of the zero-temperature parameters of

$$n(0^\circ\text{K}) = (3.33 \pm 0.03) \times 10^{18} \text{ cm}^{-3},$$

$$E_F(0^\circ\text{K}) = 22.2 \pm 0.1 \text{ meV},$$

$$\mu(0^\circ\text{K}) = -\hbar\omega_{ph}^{TO} = 1.0887 \pm 0.0001 \text{ eV},$$

$$\phi(0^\circ\text{K}) = 8.2 \pm 0.1 \text{ meV}.$$

The values of the coefficients of the T^2 terms are

$$\alpha = (1.5 \pm 0.5) \times 10^{15} \text{ cm}^{-3} \text{ }^\circ\text{K}^{-2},$$

$$\beta = (8.0 \pm 2.2) \times 10^{-3} \text{ meV } ^\circ\text{K}^{-2},$$

$$\delta = (5.9 \pm 1.1) \times 10^{-3} \text{ meV } ^\circ\text{K}^{-2}.$$

VI. DISCUSSION AND SUMMARY

In Table II we have compiled the published theoretical values of the condensate density and work function at zero temperature^{14,15,26} along with the values obtained in these experiments. The theoretical values for the condensate density which have a range of $(3.2\text{--}3.4) \times 10^{18} \text{ cm}^{-3}$ are in excellent agreement with the experimental value of $(3.33 \pm 0.03) \times 10^{18} \text{ cm}^{-3}$ obtained here. The theoretical values of the condensate work function at zero temperature range between 5.7 and 7.3 meV and are significantly lower than the experimental value of 8.2 ± 0.1 meV.

TABLE II. Parameters for the electron-hole condensate in Si obtained experimentally in this work and theoretically by other investigators.

	$n(0^\circ\text{K})$ (10^{18} cm^{-3})	$\phi(0^\circ\text{K})$ (meV)	α ($10^{15}\text{ cm}^{-3}\text{ }^\circ\text{K}^{-2}$)	β ($10^{-3}\text{ meV }^\circ\text{K}^{-2}$)	δ ($10^{-3}\text{ meV }^\circ\text{K}^{-2}$)	$\epsilon_G''(n(0))$ (10^{-37} meV cm^6)
Experimental						
This paper	3.33 ± 0.03	8.2 ± 0.1	1.5 ± 0.5	8.0 ± 2.2	5.9 ± 1.1	4.9
Theoretical						
Vashishta Das, Singwi ^a	3.2	7.3	2.4	12.3	3.8	3.17
Brinkman Rice ^b	3.4	5.7				
Combescot Nozières ^c	3.1	6.3				

^aAfter Ref. 15.^bAfter Ref. 14.^cAfter Ref. 26.

The experimental values of the coefficients of the T^2 terms along with the theoretical values of these quantities obtained by Vashishta, Das, and Singwi¹⁵ are tabulated in Table II. The theoretical values are in moderately good agreement with the experimental values.

We may further interpret the values of α , β , and δ by examining the theoretical expressions for these quantities. The slopes of the various T^2 terms are given by^{2,15,23,24}

$$\alpha = -\gamma'(n(0))/2\epsilon_G''(n(0)), \quad (10)$$

$$\beta = \frac{\pi^2 E_F(0) k_B^2}{12\epsilon_F^e(0) \epsilon_F^h(0)} - \frac{1}{3} \frac{\gamma'(n(0)) k_B^2 E_F(0)}{\epsilon_G''(n(0)) n(0)}, \quad (11)$$

and

$$\delta = \frac{1}{2} [\gamma(n(0)) k_B^2]. \quad (12)$$

In this expression $\epsilon_G''(n)$ is the second derivative of the ground-state energy of the condensate per particle, and $\gamma(n)$ is the coefficient of the T^2 term in a low-temperature expansion for the free energy per pair

$$f(T) = f(T=0^\circ\text{K}) - \frac{1}{2} \gamma(n) (k_B T)^2, \quad (13)$$

and $\gamma'(n)$ is the first derivative of $\gamma(n)$ with respect to density. In the simple free-particle model

$$\gamma(n) = \left(\frac{\pi}{3}\right)^{2/3} \left(\frac{m_{de} + m_{dh}}{\hbar^2}\right) \frac{1}{n^{2/3}}. \quad (14)$$

Using Eq. (14) and $m_{de} = 0.55m_e$, $m_{dh} = 1.08m_e$,²² and $n = 3.33 \times 10^{18}\text{ cm}^{-3}$, we have

$$\gamma_{th}(n) = 9.9 \times 10^2\text{ eV}^{-1}.$$

On the other hand, if we use Eq. (12) and the experimental value of δ we have

$$\gamma_{\text{expt}} = (1.6 \pm 0.3) \times 10^3\text{ eV}^{-1}.$$

Hence, we have that γ_{expt} is about 60% larger than γ_{th} . This discrepancy could in part be due to

mass renormalization effects in the plasma.

From the value of α and the theoretical expression for $\gamma'(n)$ obtained from Eq. (14), we may have a value for ϵ_G'' of

$$\epsilon_G''(n(0)) = 4.9 \times 10^{-37}\text{ meV cm}^6.$$

This should be compared with the theoretical value obtained by Vashishta, Das, and Singwi¹⁵ of

$$\epsilon_G''(n(0)) = 3.17 \times 10^{-37}\text{ meV cm}^6.$$

For convenience, these values are also tabulated in Table II.

Although we were unable to fit the condensate line shape above 13°K owing to interference from the free exciton, we were able to observe luminescence from the condensate at temperatures up to 17°K . This then is a lower bound on the critical temperature for the exciton-condensate phase transition T_c . We expect the critical temperature to be significantly higher than this, since our laser was able to produce exciton densities of at most 10^{17} cm^{-3} . If we take the theoretical estimates of the critical temperature 20.8 ,¹⁵ 21.6 ,²⁷ and 28°K ,²⁸ then we estimate from Eq. (6) critical densities of 2.7×10^{18} , 2.6×10^{18} , and $2.2 \times 10^{18}\text{ cm}^{-3}$. All of these values are well above the 10^{17} cm^{-3} our laser could produce.

It is important to note that the lack of temperature gradients in the experiment is crucial to the validity of the results reported here. Heating in photoluminescence experiments has been reported and also suggested as being important by several investigators in both Ge and Si.^{2,29,30} In studying the condensate luminescence in Si, the possibility of heating is greatly increased compared to Ge owing to several factors. Since the condensate density is more than an order of magnitude higher in Si than in Ge and the lifetime is more than two orders of magnitude smaller, the heat produced by

condensate recombination (mostly nonradiative) is more than three orders of magnitude higher in Si for the same condensate volume. In this work, for the reasons outlined in Sec. IV, temperature control has been adequate.

As pointed out in Sec. V, the region of discrepancy *C* of the condensate line fits in Fig. 4 has been attributed to electrons and holes recombining from the condensate and simultaneously producing excitations not described in the standard band model. Carriers which recombine in this manner will probably tend to distort the line shape in some way depending on which states are favored for this process. Thus these processes may also account for the regions of discrepancy *A* and *B* in the line fits (see Fig. 4). That these three regions of discrepancy are related is indicated also by the fact that they decrease continuously in the line fits at increasing temperatures. Although we have no understanding of the mechanism involved, it is surely significant that the differences between the calculated line shape and the experimental spectra diminish monotonically with increasing temperature.

Although not directly related to our study of the electron-hole condensate in Si, our observation of luminescence lines due to excitons bound to im-

purity sites in very high-purity Si suggests the possibility of using photoluminescence as a measure of the presence of dopant impurities in Si.

There are several important results of the electron-hole condensate line fits which substantiate the degenerate electron-hole-plasma model for the condensate in Si. First, the model gives a qualitative fit to the line shape at each temperature and excitation level. Second, the line shape displays the correct temperature dependence. That is, the high-energy side of the line is fit well at each temperature. Finally, the density, chemical potential, work function, and Fermi level each show a variation with temperature which is consistent with the T^2 dependence expected from Fermi-liquid theory. The values of the parameters characterizing the T^2 dependences are in reasonable agreement with the theoretical estimates for an electron-hole plasma in Si.

ACKNOWLEDGMENTS

The authors would like to acknowledge useful discussions with V. Marrello, R. N. Silver, and D. L. Smith. Further, the authors would like to thank G. A. Thomas for helpful comments on the manuscript.

*Work supported by the Alfred P. Sloan Foundation.

†Work supported in part by the Office of Naval Research under Contract No. N00014-75-C-0423.

¹Ya. E. Pokrovsky, Phys. Status Solidi A **11**, 385 (1972).

²G. A. Thomas, T. G. Phillips, T. M. Rice, and J. C. Hensel, Phys. Rev. Lett. **31**, 386 (1973).

³V. S. Bagaev, N. A. Penin, N. N. Sibeldin, and V. A. Tsvetkov, Fiz. Tverd. Tela **15**, 3269 (1973) [Sov. Phys. Solid State **15**, 2179 (1974)].

⁴J. M. Worlock, T. C. Damen, K. L. Shaklee, and J. P. Gordon, Phys. Rev. Lett. **33**, 771 (1974).

⁵J. C. Hensel, T. G. Phillips, and T. M. Rice, Phys. Rev. Lett. **30**, 227 (1973).

⁶J. C. McGroddy, M. Voos, and O. Christensen, Solid State Commun. **13**, 1801 (1973).

⁷V. S. Vavilov, V. A. Zayats, and V. N. Murzin, Zh. Eksp. Teor. Fiz. Pis'ma Red. **10**, 304 (1969) [JETP Lett. **10**, 192 (1969)].

⁸L. V. Keldysh, in *Proceedings of the Ninth International Conference on the Physics of Semiconductors, Moscow*, edited by S. M. Ryvkin 1968 (Nauka, Leningrad, 1968), p. 1303.

⁹G. A. Thomas, T. M. Rice, and J. C. Hensel, Phys. Rev. Lett. **33**, 219 (1974).

¹⁰J. R. Haynes, Phys. Rev. Lett. **17**, 860 (1966).

¹¹Ya. E. Pokrovsky, A. Kaminsky, and K. Svistunova, *Proceedings of the Tenth International Conference on the Physics of Semiconductors, Cambridge*, 1970, edited by S. P. Keller, J. C. Hensel, and F. Stern, CONF-700801 (U.S. AEC Div. of Tech. Information, Springfield, Va. 1970), p. 504.

¹²M. Capizzi, M. Voos, C. Benoît à la Guillaume, and

J. C. McGroddy, Solid State Commun. **16**, 709 (1975).

¹³C. Benoît à la Guillaume and M. Voos, Phys. Rev. B **7**, 1723 (1973).

¹⁴W. F. Brinkman and T. M. Rice, Phys. Rev. B **7**, 1508 (1973).

¹⁵P. Vashishta, S. G. Das, and K. S. Singwi, Phys. Rev. Lett. **33**, 911 (1974).

¹⁶K. L. Shaklee and R. E. Nahory, Phys. Rev. Lett. **24**, 942 (1970).

¹⁷T. Nishino, M. Takeda, and Y. Hamakawa, Solid State Commun. **12**, 1137 (1973).

¹⁸R. B. Hammond, D. L. Smith, and T. C. McGill, Phys. Rev. Lett. **35**, 1535 (1975).

¹⁹R. Sauer, Phys. Rev. Lett. **31**, 376 (1973).

²⁰K. Kosai and M. Gershenzon, Phys. Rev. B **9**, 723 (1974).

²¹See, for example, D. L. Goodstein, *States of Matter* (Prentice-Hall, Englewood Cliffs, N. J., 1975), p. 125.

²²R. A. Smith, *Semiconductors* (Cambridge U.P., London, 1959), p. 347-350. A number of other values of m_{de}^* and m_{dn}^* have been quoted. For example, see P. Lawaetz, Phys. Rev. B **4**, 3460 (1971). Use of the slightly different values of m_{de}^* and m_{dn}^* quoted by other sources will make changes in the results on the order of a few percent.

²³T. K. Lo, Solid State Commun. **15**, 1231 (1974).

²⁴L. D. Landau and E. M. Lifshitz, *Statistical Physics* (Pergamon, London, 1969), 2nd ed., p. 154ff.

²⁵G. G. MacFarlane and V. Roberts, Phys. Rev. **98**, 1865 (1955).

²⁶M. Combescot and P. Nozières, J. Phys. C **5**, 2369 (1972).

²⁷T. L. Reinecke and S. C. Ying, Phys. Rev. Lett. 35, 311 (1975).

²⁸M. Combescot, Phys. Rev. Lett. 32, 15 (1974).

²⁹V. S. Vavilov, E. L. Nolle, and A. Fazilov, Phys.

Status Solidi B 64, 735 (1974).

³⁰B. M. Ashkinadze, I. P. Kretsu, S. M. Ryvkin, and I. D. Yaroshetskii, Zh. Eksp. Teor. Fiz. 58, 507 (1970) [Sov. Phys.-JETP 31, 271 (1969)].